

Journal Pre-proofs

SETD7 mediates spinal microgliosis and neuropathic pain in a rat model of peripheral nerve injury

Yu Shen, Zhuofeng Ding, Shengyun Ma, Zijin Ding, Yu Zhang, Yu Zou, Fangting Xu, Xin Yang, Michael K.E. Schäfer, Qulian Guo, Changsheng Huang

PII: S0889-1591(19)30382-4
DOI: <https://doi.org/10.1016/j.bbi.2019.09.007>
Reference: YBRBI 3854

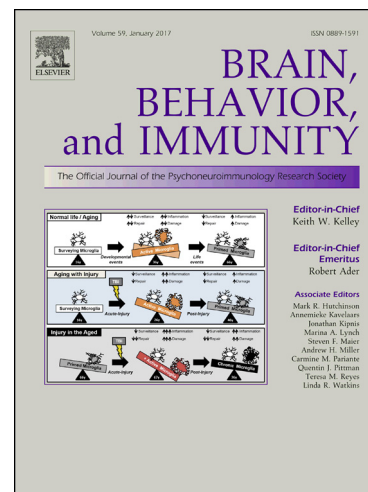
To appear in: *Brain, Behavior, and Immunity*

Received Date: 7 April 2019
Revised Date: 26 July 2019
Accepted Date: 5 September 2019

Please cite this article as: Shen, Y., Ding, Z., Ma, S., Ding, Z., Zhang, Y., Zou, Y., Xu, F., Yang, X., Schäfer, M.K.E., Guo, Q., Huang, C., SETD7 mediates spinal microgliosis and neuropathic pain in a rat model of peripheral nerve injury, *Brain, Behavior, and Immunity* (2019), doi: <https://doi.org/10.1016/j.bbi.2019.09.007>

This is a PDF file of an article that has undergone enhancements after acceptance, such as the addition of a cover page and metadata, and formatting for readability, but it is not yet the definitive version of record. This version will undergo additional copyediting, typesetting and review before it is published in its final form, but we are providing this version to give early visibility of the article. Please note that, during the production process, errors may be discovered which could affect the content, and all legal disclaimers that apply to the journal pertain.

© 2019 Elsevier Inc. All rights reserved.



SETD7 mediates spinal microgliosis and neuropathic pain in a rat model of peripheral nerve injury

Yu Shen¹, Zhuofeng Ding¹, Shengyun Ma², Zijin Ding¹, Yu Zhang¹, Yu Zou¹, Fangting Xu¹, Xin Yang¹, Michael K.E. Schäfer^{3, 4}, Qulian Guo^{1, 5}, Changsheng Huang^{* 1, 5}

Yu Shen and Zhuofeng Ding contributed equally to this work.

Author affiliations:

¹Department of Anesthesiology, Xiangya Hospital, Central South University, Changsha, China

²Department of Cellular and Molecular Medicine, University of California San Diego, La Jolla, CA, USA

³Department of Anesthesiology, University Medical Center, Johannes Gutenberg-University Mainz, Germany

⁴Focus Program Translational Neurosciences (FTN) of the Johannes Gutenberg-University Mainz, Germany

⁵National Clinical Research Center for Geriatric Disorders, Xiangya Hospital, Central South University, Changsha, China

***Corresponding author:** Changsheng Huang

Corresponding address: Department of Anesthesiology, Xiangya Hospital, Central
South University, 87 Xiangya Road, Changsha, China

E-mail address: docthuang2005@hotmail.com

Word count of the manuscript: 8781

Journal Pre-proofs

Abstract

Gene transcription regulation is critical for the development of spinal microgliosis and neuropathic pain after peripheral nerve injury. Using a model of chronic constriction injury (CCI) of the sciatic nerve, this study characterized the role of SET domain containing lysine methyltransferase 7 (SETD7) which monomethylates histone H3 lysine 4 (H3K4me1), a marker for active gene transcription. SETD7 protein expression in the spinal dorsal horn ipsilateral to nerve lesion was increased from one day to 14 days after CCI, concomitantly with the expression of inflammatory genes, *Ccl2*, *Il-6* and *Il-1 β* . The CCI-induced SETD7 expression was predominantly localized to microglia, as demonstrated by immunohistochemistry and western blot from magnetic activated cell sorted spinal microglia. SETD7 knockdown by intrathecal lentivirus shRNA delivery prior to CCI prevented spinal microgliosis and neuropathic pain, whereas lentiviral SETD7 transduction exacerbated these symptoms. In addition, SETD7 regulated H3K4me1 level and expression of inflammatory mediators both in CCI rats and in the HAPI rat microglia cell line. Accordingly, PFI-2, a specific inhibitor of SETD7 monomethylation activity, suppressed the lipopolysaccharides-induced amoeboid morphology of primary microglia and the expression of inflammatory genes, *Ccl2*, *Il-6* and *Il-1 β* . Moreover, intrathecal administration of PFI-2 alleviated CCI-induced neuropathic pain. However, this effect was observed in male but not in female rats. These results demonstrate a critical role of SETD7 in the development of spinal microgliosis and neuropathic pain subsequently to peripheral nerve injury. The pharmacological

approach further suggests that SETD7 is a new target for the treatment of neuropathic pain. The underlying mechanisms may involve H3K4me1-dependent regulation of inflammatory gene expression in microglia.

Key words: SETD7; H3K4me1; gene transcription; nerve injury; microgliosis; neuropathic pain

1. Introduction

Microglia are the resident immune cells and act as the first and main form of active immune defense in the CNS. Under healthy conditions, microglia contribute to CNS homeostasis by eliminating or remodeling synapses, scavenging the local environment for pathogens and restoring tissue integrity (Ransohoff and Perry, 2009; Shemer et al., 2015). Peripheral nerve injury could induce microgliosis in the spinal dorsal horn which has been considered a major contributor to the neuropathic pain resulting from peripheral nerve injury (Calvo and Bennett, 2012; Gu et al., 2016; Tsuda et al., 2017).

Compelling evidence was provided that the inhibition of spinal microglial response is effective in the treatment of neuropathic pain subsequent to peripheral nerve injury (Chen et al., 2018; Gu et al., 2016; Peng et al., 2016; Popiolek-Barczyk and Mika, 2016). The vast majority of identified targets are extracellular activators and their receptors in microglia, such as CX3CL1 / CX3CR1, ATP / P2X4R, IFN- γ / IFN- γ R, MCP-1 / CCR2 and LPS / TLR4 signaling, and intracellular signaling, such as JAK-STAT and P38 MAPK pathway (Calvo and Bennett, 2012; Chen et al., 2018; Ji and Suter, 2007). Besides these extracellular and intracellular signaling, the development of microgliosis requires production of inflammatory factors, including cytokines, chemokines and reactive oxygen species (Graeber et al., 2011; Harry and Kraft, 2008). The production of these factors depends on the regulation of gene transcription, whose activity is mostly determined by nuclear chromatin mechanism (Remenyi et al., 2004; Zhu et al., 2012) such as posttranslational modifications on

histones (Bannister and Kouzarides, 2011; Peterson and Laniel, 2004; Zhang and Dent, 2005). Histone modifications, e.g. methylation, acetylation, and ubiquitination, regulate the accessibility of transcription complexes and chromatin remodelers. Accordingly, a large number of histone modifying enzymes have been shown to regulate gene transcription (Marmorstein and Trievel, 2009).

SET domain containing lysine methyltransferase 7 (SETD7, also known as SET7/9, KIAA1717, KMT7, SET7, SET9) was the first lysine methyltransferase discovered to monomethylate histone H3 lysine 4 (H3K4me1), a marker of enhancer required for gene transcription (Bulger and Groudine, 2011; Nishioka et al., 2002; Rice et al., 2003). SETD7 and associated H3K4me1 have been shown to regulate the transcription of inflammatory genes. For example, SETD7-mediated H3K4me1 at promoters of inflammatory genes, such as *Ccl2* (*MCP-1*), *Tnf- α* , and *Il-8*, increases recruitment and stability of the NF κ B-p65 subunit (Ea and Baltimore, 2009; Li et al., 2008). In addition, functional studies in monocytes and macrophages revealed that suppression of SETD7 is sufficient to block the expression and release of inflammatory factors (He et al., 2015; Li et al., 2008). These findings suggest that inflammatory responses of other cell types such as microglia, which show many similarities with macrophages (Ginhoux et al., 2010), may also depend on SETD7.

To test the hypothesis that SETD7 regulates inflammatory responses of microglia, we subjected rats to the chronic constriction injury (CCI) model of peripheral nerve injury which evokes spinal microgliosis and associated neuropathic pain (Mika et al., 2009; Xu et al., 2016a). We examined the spinal expression regulation and cellular

localization of SETD7 after CCI by immunohistochemistry, western blot of ipsilateral spinal dorsal horn lysates and magnetic-activated cell sorting of spinal microglia. The functional role of SETD7 in the development of spinal microgliosis, neuropathic pain and underlying regulation of H3K4me1 and inflammatory gene transcription, was determined by virus-mediated genetic knockdown or overexpression approaches, respectively. Finally, pharmacological inhibition experiments using the specific SETD7 monomethylation activity inhibitor PFI-2 (Barsyte-Lovejoy et al., 2014) were performed in primary microglia and CCI followed by gene expression and behavioral analyses, respectively.

2. Materials and Methods

2.1 Animals

Adult Sprague–Dawley (SD) rats were obtained from Hunan SLAC Laboratory Animal Co., LTD., Changsha, China. We used the minimum number of rats in the allowed range, in accordance with the Guide for the Care and Use of Laboratory Animals (US National Research Council, 1996). All the in vivo experiments were performed in male rats, except the experiment of pharmacological inhibition of SETD7 which was performed both in male and female rats. Rats were housed in a temperature (25–28°C) and humidity-controlled environment and specific pathogen free room with a 12-hr light/ dark cycle and free access to food and water. All procedures were approved by Institutional Ethics Committee of Xiangya Hospital, Central South University and carried out in accordance with the National Institutes of

Health guide for the care and use of Laboratory animals.

2.2 Rat model of CCI

CCI was performed according to the procedure of Bennett and Xie (Bennett and Xie, 1988). In brief, under anesthesia with isoflurane, the left sciatic nerve was exposed after blunt separation from the surrounding tissue. Four snug ligatures (4–0) were tied around the nerve at 1-mm intervals. All nerve ligations were conducted by one person to control the same tightness of ligation. The nerve was placed in situ in the intramuscular spaces after ligation and skin wounds were closed. For the sham surgery, the sciatic nerve was exposed but without ligation.

2.3 Behavioral assessment

Rats were randomized to different groups and examined on the same day according to a random number table generated by a person who was not involved in this study. All measurements were carried out by investigators blind to the experimental groups.

The mechanical withdrawal threshold (MWT) on the ipsilateral paw was determined using von Frey filaments (North Coast Medical, San Jose, CA) as described in our previous study (Xu et al., 2018). In brief, rats were placed in a plastic chamber with a mesh floor to separate with each other and allowed to acclimate for 30 minutes. The stimuli was applied on the lateral side of the plantar surface of the ipsilateral paw with von Frey filaments ranging from 0.4g to 15g. The stimuli force was applied using up and down method and calculated as MWT.

The thermal withdrawal latency (TWL) on the ipsilateral paw was tested using a thermal pain test instrument (Tes7370, Ugo Basile, Comerio, Italy) (Xu et al., 2018). Briefly, rats were placed in an individual chamber on the heat conductive glass plate and habituated for 30 minutes before test. Heat stimuli with a cutoff time set at 30 seconds (s) was applied on the plantar surface of hind-paw for three times with a 5 minutes interval. The three latencies when the paw moved were recorded and averaged as TWL.

2.4 Construction of lentiviral vectors

The nucleotide sequences for the siRNA to knockdown the rat *SETD7* gene (NM_001109558.1), and for the non-silencing control siRNA were as follows: shSETD7, GGAAATTCTTCTTCTTTGA; negative control siRNA, TTCTCCGAACGTGTCACGT. Then the oligonucleotides containing silencing siRNA or negative control siRNA sequences were constructed into the plasmid H1 / GFP&Puro, respectively. The packaged plasmids (Suzhou Genepharma Co. China) were then cloned into the lentiviral vector LV3 (Suzhou Genepharma Co. China), and the recombinant lentiviral vectors were designated as LV-shRNA-SETD7 and LV-NC. The lentiviral vector-mediated overexpression of SETD7 (LV-SETD7) was accomplished by inserting *SETD7* (NM_001109558.1) encoding cDNAs into EF-1aF / GFP&Puro plasmid (Suzhou Genepharma Co. China), and cloned into the lentiviral vector LV5 (Suzhou Genepharma Co. China). The same vector backbone that did not express SETD7 but carried the GFP gene was used to generate a control lentivirus

(control). The lentiviral expression vectors and packaging plasmids were co-transduced into 293T human embryonic kidney (HEK) cells (supplier) using RNAi-Mate solution (Suzhou Genepharma Co. China) to generate the recombinant lentivirus mentioned above. The viral particles were collected and the titer was determined at 72 hours after transfection. The final titer was adjusted to 1×10^9 TU/ml.

2.5 HAPI microglia cell line

The rat microglia cell line HAPI (Huiying biological Technology CO., LTD, Shanghai, China) (Cheepsunthorn et al., 2001) was cultured in complete RPMI 1640 medium with 10% (v/v) fetal bovine serum and 1% (v/v) penicillin and streptomycin (Thermo Fisher Scientific, Waltham, MA) at 37°C with 5% CO₂ in incubator. The cells were passaged at 2 days interval and the medium was changed every day. To determine the optimal lipopolysaccharides (LPS) dose, cells were treated with 0.1, 1, and 10 µg/ml LPS (Sigma-Aldrich, USA). Expression of SETD7 was silenced by transfection of LV-shRNA and overexpressed by transfection of LV-SETD7. LV-NC and GFP control were also transfected to generate the control cell lines, respectively. Cells were treated with 2 µg/ml puromycin (Sigma-Aldrich, USA) for positive selection of transfected cells. Cells were cultured for 24 hours after LPS administration and total RNA and proteins were extracted for further analysis.

2.6 Magnetic activated cell sorting

Magnetic activated cell sorting (MACS) was performed using fetal rat brain and

ipsilateral spinal dorsal horn of sham-operated and CCI rats at 7 days post injury. Animals (18-day pregnant female SD rat and CCI or sham-operated adult rats) were anesthetized with isoflurane, followed by brain and spinal cord dissection of the fetal brains and the ipsilateral spinal dorsal horn of adult rats, respectively. The meninges were removed from the brains and tissues which was dissociated by enzymatic digestion using the Neural Tissue Dissociation Kit P (Miltenyi Biotec, Bergisch Gladbach, Germany) as described (Holt and Olsen, 2016), and 0.4 grams of tissue was processed for each sample using gentleMACS C tube (Miltenyi Biotec, Bergisch Gladbach, Germany). Dissociated cell mixtures of the ipsilateral spinal dorsal horn from six rats were combined and myelin debris was removed using Myelin Removal Beads (Miltenyi Biotec) and Debris Removal Solution (Miltenyi Biotec). CD11b/c MicroBeads were added to sort microglia from the cell mixtures from adult spinal cord or fetal brain, and subjected to magnetic separation, according to the manufactures instruction (Miltenyi Biotec). The anti-CD11b/c sorted microglia (positive fraction) and the microglia depleted fraction (negative fraction) from the ipsilateral spinal dorsal horn were snap frozen in liquid nitrogen and stored at -80°C until further biochemical analysis. The CD11b/c sorted microglia from the fetal rat were used for primary microglial culture.

2.7 Primary microglia

Primary rat microglia were purified by MACS as described above. The cells were resuspended in Microglia Medium (MM, ScienCell, USA) including 20%

heat-inactivated Fetal Bovine Serum (FBS, ScienCell, USA), 1% (v/v) penicillin and streptomycin (P/S, ScienCell, USA), and 1% (v/v) Microglia Growth Supplement (MGS, ScienCell, USA). Cells were seeded in a 24-well plate and cultivated for two days until they adhered to the plate bottom. The purity of the isolated microglia was determined by immunocytochemistry using anti-Iba1 (1:200; Abcam, MA, USA). The primary microglia were subjected to the following treatment: (i) 0.1 µg/ml LPS for 12h, (ii) pretreatment with 0.1 µmol PFI-2 (Selleck, Shanghai, China), a specific inhibitor of SETD7 monomethylation activity (Baryte-Lovejoy et al., 2014) for 2h then followed by 0.1 µg/ml LPS for 12h, and (iii) 0.1% (v/v) dimethyl sulfoxide (DMSO, vehicle) pre-treatment for 2h then followed by 0.1 µg/ml LPS for 12h, respectively. The dose of PFI-2 was chosen according to a previous study (Baryte-Lovejoy et al., 2014). Microglia without treatment (blank) were used as control.

2.8 Intrathecal delivery of lentiviral vectors or drugs

The intrathecal catheter implantation was carried out according to our previous study (Ding et al., 2017). Briefly, under anesthesia with isoflurane, rat was placed in a position in which the lumbar vertebra arched back and lumbar intervertebral space was exposed. A PE-10 catheter was then implanted into the subarachnoid space between the L4 and L5 intervertebral space and the leakage end of the catheter was fixed in the neck under a subcutaneous tunnel. After recovery for 3 days, a lidocaine test was administrated to confirm the correct position of the catheter. Briefly, the

bilateral hind limbs of rat were paralyzed within 30 s after injection of 2% lidocaine (10 μ l) through a successfully placed intrathecal catheter. Then, it was recovered 30 min after that. Only rats with a successful placement of intrathecal catheter were used for further investigations.

Rats received LV-shRNA, LV-NC (10 μ l, 1×10^9 TU/ml) or 10 μ l sterile saline via intrathecal catheter 7 days before the CCI surgery ($n = 8$ for each group). Rats in the sham operation group were administered with 10 μ l sterile saline as a control via intrathecal injection ($n = 8$). Naive rats were randomly divided into two groups ($n = 8$ for each group) and intrathecally injected LV-SETD7 or control lentivirus, respectively. The MWT and TWL were measured before and after intrathecal injection or CCI modeling.

For the pharmacological treatment experiments, rats with successful intrathecal catheter were randomly divided into five groups ($n = 6$ for each group), among which four groups of rats received CCI surgery and one group received sham surgery. PFI-2 was diluted in 10 μ l 0.1% (v/v) DMSO (vehicle) to a concentration of 1 μ mol, 4 μ mol, or 10 μ mol, respectively. The sham-operated rats and one group of CCI rats received only vehicle treatment. The other three groups of CCI rats received 1 μ mol, 4 μ mol, or 10 μ mol PFI-2, respectively. The drug or vehicle was injected intrathecally once daily from the day when the CCI or sham surgery was performed to the next 14 days. The MWT and TWL were measured before and at 1 day (d), 3 d, 7 d, and 14 d after intrathecal injection or CCI.

2.9 Immunofluorescence and microscopy

Immunofluorescence analysis was performed using HAPI microglia cell line, primary microglia and rat spinal cord sections. For spinal cord immunohistochemistry, rats were anesthetized with overdosed pentobarbital sodium (100 mg/kg, i.p.) and infused with phosphate-buffered saline (1 M, pH 7.4) and 4% paraformaldehyde through the left ventricle of the heart. The lumbar spinal cord was dissected out and post-fixed in 4% paraformaldehyde for 8h at 4°C, then transferred to 15% and 30% sucrose at 4°C for 24 hours. 10- μ m transverse frozen sections were cut and collected.

Cells or spinal cord sections were washed with PBS/0.3% Triton X-100 (PBST, Sigma, St. Louis, MO, USA) three times, each for 10 min, and blocked with 5% (v/v) donkey serum in PBST for 1 hour, followed by incubation with primary antibodies: rabbit anti-SETD7 (1:100, Abcam, MA, USA), rabbit anti-SETD7 (knockout-validated, 1:100, ABclonal, Wuhan, China), mouse anti-CD11b (1:100; Abcam, MA, USA), mouse anti-NeuN (1:400; Abcam, MA, USA), mouse anti-Iba-1 (1:400; Abcam, Cambridge, UK), mouse anti-GFAP (1:400; Cell Signaling Technology, MA, USA) and rabbit anti-H3K4me1 (1:200, Cell Signaling Technology, MA, USA) at 4°C for 16h. Sections were washed three times in PBST and incubated with secondary antibodies conjugated with Alexa 488 (donkey anti-mouse, 1:200; donkey anti-rabbit, 1:200; Jackson ImmunoResearch Laboratories, West Grove, PA, USA) or Alexa 594 (donkey anti-rabbit, 1:300; donkey anti-mouse, 1:400; Jackson ImmunoResearch Laboratories) for 2 hours at 4°C. After washing three times in PBST, sections were sealed and images were captured with identical acquisition parameters for each

immunostaining using a Leica DM5000B microscope (Leica biosystems, Wetzlar, Germany) or an automatic digital slide scanner (Pannoramic MIDI, 3D HISTECH, Budapest, Hungary). The acquisition of images and quantitative analysis of the immunofluorescence staining were performed by an investigator blind to experimental groups. Three sections per animal were used for quantitative analysis for each staining. The number cells were counted in the ipsilateral spinal dorsal horn as described (Huang et al., 2016). The immunofluorescence density was evaluated using Image Pro Plus 6.0 (Ding et al., 2018).

2.10 Western blot

Western blot analysis was performed using lysates from HAPI cells, tissues and MACS-isolated cells from the spinal dorsal horn ipsilateral to the affected sciatic nerve and tissues from the ipsilateral L4-L5 dorsal root ganglions (DRGs), respectively. The cells and tissues were homogenized using the Nuclear and Cytoplasmic Protein Extraction Kit (TransGen Biotech, Beijing, China) to extract the nuclear fractions according to the operating instruction manual. Protein samples were concentrated by BCA assay and heated at 99°C for 10 min. Denatured protein samples (50 µg per lane) were separated by 12% SDS-PAGE gel electrophoresis, transferred to Immun-Blot PVDF membranes (Millipore, MA) and blocked with 5% bovine serum albumin for 2 hours at room temperature and then incubated with antibodies rabbit anti-SETD7 (1:500, Abcam, MA, USA), mouse anti-H3K4me1 (1:1000, Active Motif, CA, USA), mouse anti-H3K4me3 (1:1000, Active Motif, CA, USA), mouse

anti-H3K27ac (1:1000, Active Motif, CA, USA), rabbit anti-CD11b (1:1000, Abcam, MA, USA) and mouse anti-H3 (1:1000, Cell Signaling Technology, MA, USA) at 4°C overnight. Membranes were washed and incubated with horseradish peroxidase (HRP) conjugated secondary mouse or rabbit antibody (1:5000, Jackson ImmunoResearch Lab, PA, USA) for 2 hours at room temperature. Protein bands were visualized using an ECL Plus blot kit (Merck Milipore, Hercules, USA) and scanned with a ChemiDoc XRS System using Image Lab software (Bio-Rad, Universal Hood III, USA). Band intensities of the SETD7 and H3K4me1 were normalized to that of H3, respectively.

2.11 Enzyme-linked immunosorbent assay

Tissues from the ipsilateral spinal dorsal horn was dissected, homogenized in a tissue grinder and after disrupting the cell membrane by repeated freeze-thaw treatment, the tissue homogenate was centrifuged at 5000g for 2 minutes at 4°C for 5 minutes. Protein concentration was determined in the supernatant using a BCA Protein Quantitative Kit (TransGen Biotech, Beijing, China), then diluted to a final concentration of 1 mg/mL. Samples were subjected to enzyme-linked immunosorbent assay to determine protein levels of MCP-1 (CCL2) (Cusabio Biotech, Wuhan, China), interleukin-6 (IL-6) (Cusabio Biotech), and interleukin-1 β (IL-1 β) (Proteintech, Wuhan, China) according to the manufacturer`s protocols. Signals were quantified with the Multiskan Spectrum full wavelength microplate reader (Thermo Fisher Scientific, Grand Island, NY).

2.12 Real-time quantitative polymerase chain reaction

Real-time quantitative polymerase chain reaction (RT-qPCR) was performed using HAPI cells, primary microglia or tissues from the spinal dorsal horn ipsilateral to the affected sciatic nerve, respectively. Total RNA was isolated from cells and tissues using the E.Z.N.A. Total RNA Kit (Omega, Shanghai, China) and subjected to cDNA synthesis using the PrimeScript RT reagent Kit (Takara, Otsu, Japan), according to the manufacturer's instructions. RT-qPCR was prepared with a Quantifast SYBR Green PCR Kit (GeneScript, Guangzhou, China). The following target genes were examined: *SETD7*, *Ccl2*, *Il-6*, *Il-1 β* and *β -Actin* (all primer sequences are listed in Supplemental Table 1). RT-qPCR was performed with an ABI Prism 7300 PCR System (Applied Biosystems) using the PCR cycling parameter setting as 95°C for 10 min, followed by 40 cycles of 95°C for 15 s, 60°C for 25 s, and 72°C for 24s. Relative expression of the target genes compared to *β -Actin* probed as endogenous reference gene were calculated using the $\Delta\Delta$ Ct method.

2.13 Statistical analysis

All data are presented as mean \pm SD. Shapiro-Wilk test was used to test for data distribution. For analyses of datasets with parametric distribution, two-tailed unpaired Student's t test was used for comparisons between two groups and one-way or two-way ANOVA with Bonferroni multiple comparison test was used for comparisons among multiple groups. For the analysis of datasets with non-parametric distribution, the Mann-Whitney U test was used for comparisons between two groups and the

Kruskal–Wallis test with Dunn’s multiple comparisons post-test was used for comparisons among multiple groups. $p < 0.05$ was considered to be statistically significant. All statistical analyses were conducted using SPSS 18.0 (SPSS Inc., Chicago, Illinois, USA) and GraphPad Prism 7.0 (GraphPad Software Inc., San Diego, California, USA).

3. Results

3.1 CCI induces neuropathic pain and up-regulates expression of SETD7 protein and inflammatory genes in spinal dorsal horn ipsilateral to nerve lesion

Rats developed neuropathic pain after CCI, which manifested as the decrease of MWT and TWL in the ipsilateral paw from 3 days (d) to 14d after CCI (compared to sham-operated rats, for MWT $p < 0.05$ at 3d and $p < 0.001$ from 7d to 14d after CCI, for TWL $p < 0.01$ at 3d and $p < 0.001$ from 7d to 14d after CCI, Fig. 1A, B). To characterize the role of SETD7 in the CCI model, we first evaluated the overall expression of SETD7 protein in the ipsilateral spinal dorsal horn and L4-L5 DRGs at several consecutive time points, including 12 hours (h), 1d, 3d, 7d and 14d after sham or CCI surgery by western blot. Compared to sham-operated rats, SETD7 in the ipsilateral spinal dorsal horn was significantly increased as early as 1d after CCI and the increase was sustained until 14d after CCI, the endpoint of our study ($p < 0.05$ at each time point from 1d to 14d, Fig.1C). In contrast, SETD7 in the ipsilateral L4-L5 DRGs was not altered at the time points investigated after CCI (Fig.1D).

We further determined the expression of the inflammatory genes *Ccl2*, *Il-6* and *Il-1 β*

in the ipsilateral spinal dorsal horn by RT-qPCR. Compared to their gene expressions in sham-operated rats, *Ccl2*, *Il-6* and *Il-1 β* were significantly increased from 1d to 14d after CCI (compared to sham-operated rats, for *Ccl2* $p < 0.01$ from 1d to 3d and $p < 0.001$ from 7d to 14d after CCI, for *Il-6* $p < 0.05$ from 1d to 14d after CCI, for *Il-1 β* $p < 0.01$ at 1d, $p < 0.05$ at 3d, $p < 0.001$ at 7d and $p < 0.05$ at 14d after CCI, Fig. 1E). These results showed a similar regulation pattern of SETD7 protein and *Ccl2*, *Il-6* and *Il-1 β* gene after CCI, suggesting a potential role of SETD7 in regulating the transcription of these inflammatory genes.

3.2 CCI-induced expression of SETD7 protein is localized to ipsilateral spinal dorsal horn microglia

In agreement with previous studies (Mika et al., 2009; Xu et al., 2016a), CCI induced microgliosis in the spinal dorsal horn ipsilateral to the nerve lesion. Immunohistochemistry demonstrated microglial proliferation and morphological transformation from ramified cells (sham-operated rats) to hypertrophied and amoeboid cells (CCI rats, representative images from 7d after CCI, Fig. 2A).

To explore the SETD7 function in spinal microgliosis and neuropathic pain, we conducted immunofluorescence staining of SETD7 in the rat lumbar spinal cord at 7d post injury, when the CCI-induced neuropathic pain has been already manifested (Xu et al., 2016a). To ensure specificity of SETD7 immunostaining, two different antibodies were used (rabbit anti-SETD7, Abcam, MA, USA and knockout-validated rabbit anti-SETD7, ABclonal, Wuhan, China). In both the sham-operated rats and

CCI rats, SETD7 was highly co-localized with NeuN and GFAP protein, which are markers of neurons and astrocytes, respectively (Supplemental Fig. 1). Surprisingly, there was limited co-localization of SETD7 with the microglia marker Iba1 in sham-operative rats. However, SETD7 was highly expressed in microglia after CCI (Fig. 2A and Supplemental Fig. 2). Specifically, $59.8 \pm 21.9\%$ of microglia showed SETD7 positive staining in the ipsilateral spinal dorsal horn of sham-operative rats. After CCI, the ratio increased up to $93.8 \pm 2.1\%$ ($p < 0.01$, compared to sham-operated rats, Fig. 2B). Compared to the sham-operated rats, a stronger appearance of SETD7 immunostaining was observed in the nuclei of microglia after CCI (Fig. 2C). Thus, immunohistochemistry indicated an increase of SETD7 expression in microglia in the spinal dorsal horn ipsilateral to CCI.

To confirm this finding, we performed a MACS isolation of microglia at 7d post sham and CCI using CD11b/c MicroBeads and examined the SETD7 protein expression. Western blot analysis confirmed high enrichment of CD11b protein in the positive fraction, whereas the negative fraction was almost devoid of CD11b protein (Fig. 2D). SETD7 protein was significantly higher in the positive fraction of CCI rats compared to that of sham-operated rats ($p < 0.001$, Fig. 2D). In contrast, the amount of SETD7 protein in the negative fraction did not differ between the sham-operated rats and the CCI rats. These results, together with the immunohistochemical observations, showed that CCI induced an up-regulation of SETD7 protein in microglia in the spinal dorsal horn ipsilateral to the nerve lesion.

3.3 SETD7 knockdown suppresses spinal microgliosis and alleviates CCI-induced neuropathic pain

In order to investigate the relevance of SETD7 for spinal microgliosis and associated neuropathic pain after CCI, we knocked down SETD7 using LV-shRNA prior to CCI. The LV-shRNA was delivered to the spinal cord via an intrathecal catheter 7 days before sham or CCI surgery. Immunofluorescence staining demonstrated successful LV infection of cells in the spinal dorsal horn including microglia (Supplemental Fig. 3).

At 14d after surgery, ipsilateral spinal dorsal horns were processed for further analyses. Compared to LV-NC, LV-shRNA prevented the CCI-induced increase of SETD7 protein in the ipsilateral spinal dorsal horn ($p < 0.05$, Fig. 3A). Moreover, SETD7 knockdown dramatically suppressed microgliosis in the ipsilateral spinal dorsal horn, as indicated by the decrease of Iba1-labeled, activated microglia in this region (CCI + NS vs sham + NS, $p < 0.05$; CCI + LV-shRNA vs CCI + LV-NC, $p < 0.05$, Fig. 3B). This result was confirmed by immunostaining with antibodies specific for CD11b, another marker of activated microglia (Supplemental Fig. 4). In addition, SETD7 knockdown attenuated the CCI-induced expression of the inflammatory mediators, CCL2, IL-6 and IL-1 β (CCI + NS vs sham + NS, $p < 0.01$ for CCL2, $p < 0.001$ for IL-6 and IL-1 β ; CCI + LV-shRNA vs CCI + LV-NC, $p < 0.01$ for CCL2, IL-6 and IL-1 β , Fig. 3C).

To examine consequences on neuropathic pain, we further assessed MWT and TWL at different time points after CCI. Compared to LV-NC, CCI rats receiving SETD7

LV-shRNA displayed a significant increase of MWT at 3d ($p < 0.05$), 7d ($p < 0.001$), 10d ($p < 0.05$) and 14d ($p < 0.01$), and TWL also at 3d ($p < 0.01$), 7d ($p < 0.01$), 10d ($p < 0.05$) and 14d ($p < 0.001$, Fig. 3D). These data demonstrate that SETD7 knockdown alleviated CCI-induced neuropathic pain.

3.4 SETD7 overexpression causes spinal microgliosis and pain hypersensitivity in naive rats

We next tested the hypothesis that increased level of SETD7 may aggravate microgliosis and neuropathic pain after CCI. To this end, we transduced LV-SETD7 in the lumbar spinal cord of naive rats via intrathecal injection. Compared to control, transduction of LV-SETD7 caused a remarkable increase of SETD7 protein in the spinal dorsal horn ($p < 0.05$, Fig. 4A) Furthermore, the Iba1-immunolabeling of microglia in the spinal dorsal horn were increased after SETD7 overexpression ($p < 0.01$, Fig. 4B). Similar effects were found for CD11b immunolabeling (Supplemental Fig. 5). Furthermore, MWT on the hind paw were decreased from 5d to 14d after LV-SETD7 transfection ($p < 0.001$), and the TWL were decreased from 10d to 14d after LV-SETD7 transfection (after 10d, $p < 0.001$, after 14d, $p < 0.01$), respectively (Fig. 4C). Together, these results show that SETD7 overexpression aggravates spinal microgliosis, as well as mechanical and thermal pain hypersensitivity in naive rats.

3.5 SETD7 up-regulates monomethylation level of H3K4 in ipsilateral spinal dorsal horn microglia after CCI

To examine the mechanisms underlying SETD7-mediated microgliosis and neuropathic pain, we next studied the CCI-induced modifications of histone lysine after CCI. These modifications, including H3K4me1, histone H3 lysine 4 trimethylations (H3K4me3) and histone H3 lysine 27 acetylation (H3K27ac), have been involved in the regulation of gene expression (Calo and Wysocka, 2013; Dong and Weng, 2013; Heintzman et al., 2007). Similar to the changes in SETD7 expression, the level of H3K4me1 in the ipsilateral spinal dorsal horn was up-regulated from 1d to 14d after CCI (compared to sham-operated rats, $p < 0.05$ at each time point from 1d to 14d, Fig. 5A, B). However, CCI did not alter the histone lysine modification levels of H3K4me3 or H3K27ac at any of the time points investigated after CCI (Fig. 5A, C, D). In contrast to increased H3K4me1 level in the ipsilateral spinal dorsal horn, the H3K4me1 level was not affected by CCI in the ipsilateral L4-L5 DRGs (Supplemental Fig. 6).

The cellular expression pattern of H3K4me1 in the ipsilateral spinal dorsal horn also showed a change similar to that of SETD7 after CCI. In both the sham-operated rats and CCI rats, H3K4me1 was highly co-localized with NeuN-immunolabeled neurons and GFAP-immunolabeled astrocytes (Supplemental Fig. 7). In sham-operated rats, the ratio of H3K4me1 / Iba1 positive (H3K4me1⁺ / Iba1⁺) microglia was $45.2 \pm 17.6\%$. After CCI, the ratio of H3K4me1⁺ / Iba1⁺ microglia was strongly increased to $90.3 \pm 4.3\%$ (compared to sham-operated rats, $p < 0.001$, representative images from 7d after sham-operated and CCI modeling, Fig. 5E, F).

Moreover, the level of H3K4me1 was also examined in the MACS-isolated positive

fraction and negative fraction from the ipsilateral spinal dorsal horn at 7d after CCI. Similar to SETD7, the amount of H3K4me1 protein was significantly higher in the positive fraction from CCI rats compared to that of sham-operated rats ($p < 0.01$, Fig. 5G). In contrast, H3K4me1 level in the negative fraction did not differ between the sham-operated rats and the CCI rats (Fig.5G). Taken together, these results showed that H3K4me1 level is increased subsequently to CCI in the ipsilateral spinal dorsal horn microglia.

In the ipsilateral spinal dorsal horn, H3K4me1 was co-localized with SETD7 (Fig. 5H) and SETD7 knockdown using LV-shRNA significantly attenuated the CCI-induced increase of H3K4me1 level (Compared to CCI + LV-NC, $p < 0.05$, Fig. 5I). Conversely, SETD7 overexpression using LV-SETD7 increased the H3K4me1 level in naive rats (compared to control, $p < 0.05$, Fig. 5J).

In addition to SETD7, other histone modifying enzymes may regulate H3K4me1 level. These include lysine-specific demethylase 1 (LSD1) which specifically removes histone H3K4me2 to H3K4me1 or H3K4me0 (Maiques-Diaz and Somervaille, 2016), and mixed lineage leukemia (MLL) family proteins (Xu et al., 2016b). However, our results do not support a role of these enzymes in the regulation of H3K4me1 level in microglia (Supplemental Fig. 8 and Supplemental Fig. 9).

3.6 SETD7 controls monomethylation level of H3K4 and inflammatory gene expression in microglia

Next, we examined whether SETD7-dependent modification of H3K4me1 may

enhance expression of inflammatory mediators in microglia. As immunostaining of pro-inflammatory cytokines and chemokines in CNS tissues is often hampered by low expression levels and the lack of specific antibodies under these conditions, we took advantage of both the HAPI microglia cell line and primary microglia.

HAPI cell is a rat microglial cell line (Cheepsunthorn et al., 2001), as confirmed by Iba-1 immunostaining (Fig. 6A). SETD7 was knocked down by LV-shRNA in HAPI cell (compared to CCI + LV-NC, $p < 0.001$, Fig. 6B) prior to their stimulation using LPS. SETD7 knockdown prevented the LPS-induced up-regulation of H3K4me1 level in HAPI microglia (LPS + LV-shRNA vs LPS + LV-NC, $p < 0.01$, Fig. 6C). The LPS-induced expression of microglia-related inflammatory genes, *Ccl2*, *Il-6* and *Il-1 β* , were also attenuated by LV-shRNA (Compared to LPS + LV-NC, $p < 0.05$, Fig. 6D). SETD7 was then overexpressed in HAPI microglia by LV transfection (LV-SETD7). Compared to the control, LV-SETD7 significantly enhanced the level of SETD7 and H3K4me1 ($p < 0.01$, Fig. 6E). The gene expression of *Ccl2*, *Il-6* and *Il-1 β* were also up-regulated by LV-SETD7 (for *Ccl2*, $p < 0.001$, for *Il-6* and *Il-1 β* , $p < 0.01$, Fig. 6F).

We then examined whether SETD7 monomethylation activity regulates expression of inflammatory mediators in primary microglia. Primary microglia were isolated from fetal rats using MACS (Supplemental Fig. 10). LPS induced a morphological transformation in primary microglia, from ramified cells (sham-operated rats) to amoeboid cells (CCI rats) (Fig.7A). Treatment with PFI-2, a specific inhibitor of SETD7 monomethylation activity (Barsyte-Lovejoy et al., 2014), prevented the LPS-induced microglial morphological change and the LPS-induced expression of

inflammatory genes, *Ccl2*, *Il-6* and *Il-1 β* . (PFI-2 + LPS vs Vehicle + LPS, for *Ccl2*, $p < 0.01$, for *Il-1 β* and *Il-6*, $p < 0.001$, Fig. 7 B). These results indicated that the monomethylation activity of SETD7 regulates expression of inflammatory genes in microglia.

3.7 Inhibition of SETD7 monomethylation activity alleviates CCI-induced neuropathic pain

Finally, to evaluate the therapeutic value of targeting SETD7, we treated CCI rats with PFI-2 to test whether SETD7 monomethylation activity is involved in the development of neuropathic pain. The daily intrathecal injection of PFI-2 in a dose of 1 μmol did not affect the MWT and TWL in CCI rats (Fig. 8A, B). Compared to rats received vehicle, PFI-2 in a dose of 4 μmol showed an analgesic effect only on the TWL 14d after CCI ($p < 0.001$, Fig. 8A, B). The most significant analgesic effect of PFI-2 was observed in a dose of 10 μmol , which led to an increase of MWT at 3d ($p < 0.01$), 7d ($p < 0.01$) and 14d ($p < 0.01$, Fig. 8A), and TWL also at 7d ($p < 0.001$) and 14d ($p < 0.001$, Fig. 8B) after CCI, respectively. These results demonstrate that PFI-2 alleviated the CCI-induced neuropathic pain in a dose-dependent manner. Considering these results were obtained in male rats, we also evaluated whether PFI-2 is effective in treatment of neuropathic pain in female rats. However, in contrast to the analgesic effect in male rats, PFI-2 in a dose of 10 μmol did not alter the MWT and TWL in female rats at any of the time points investigated after CCI (Supplemental Fig. 11). These results indicate that PFI-2 alleviated the CCI-induced neuropathic pain

in male but not in female rats.

4. Discussion

In this study we provide first evidence that SETD7 is involved in the development of spinal microgliosis and neuropathic pain in a rat CCI model of peripheral nerve injury. We investigated early events up to 14 days after CCI. We found that CCI led to increased SETD7 expression, microgliosis and the induction of inflammatory gene expression in the ipsilateral spinal dorsal horn and increasing signs of neuropathic pain. SETD7 knockdown or overexpression inhibited or induced spinal microgliosis and rat pain hypersensitivity, respectively. SETD7 up-regulated H3K4me1 level in spinal microglia after CCI and also regulated H3K4me1 level and expression of inflammatory genes in HAPI microglia. Finally, pharmacological inhibition of SETD7 monomethylation activity with PFI-2 alleviated CCI-induced neuropathic pain.

The mechanism contributing to increased SETD7 expression after CCI are elusive. However, the increase of SETD7 has been previously reported in proliferated or differentiated cells, such as several kinds of tumor cells (Chen et al., 2016; Duan et al., 2018; Montenegro et al., 2016) or stem cells (Judson et al., 2018; Tuano et al., 2016), indicating its expression could be regulated by cell differentiation or pluripotency factors (Tao et al., 2011; Tuano et al., 2016). Neurons and astrocytes do not show obvious proliferation in the spinal cord especially during the early stage after peripheral nerve injury (Graeber et al., 1988; Gu et al., 2016; Ji et al., 2006;

Liu et al., 2000) and microglia are considered the most proliferative cells in spinal cord in response to peripheral nerve injury (Gu et al., 2016). The activation and proliferation of resident microglia instead of infiltrated macrophage contribute to peripheral nerve injury-induced microgliosis in the spinal dorsal horn (Denk et al., 2016; Gu et al., 2016). Thus, SETD7 may be involved in proliferation signaling and increased expression along with microgliosis after CCI.

SETD7 is a major histone methyltransferase catalyzing H3K4me1 (Nishioka et al., 2002). We found the level of H3K4me1 in the ipsilateral spinal dorsal horn microglia was increased after CCI. SETD7 knockdown or overexpression led to a corresponding down-regulation or up-regulation of H3K4me1 in both the rat spinal cord and the HAPI microglia cell line. These results indicated that SETD7 may mediate the H3K4me1 level in microglia. H3K4me1 is a marker of enhancer which is critical for gene expression in eukaryotes (Bulger and Groudine, 2011; Nishioka et al., 2002; Rice et al., 2003). We showed that the increase of SETD7 and H3K4me1 level was associated with an up-regulation of gene expression of inflammatory mediators, including *Ccl2*, *Il-6* and *Il-1 β* , from one day to 14 days after CCI. SETD7 knockdown reversed the CCI-induced expression of these inflammatory mediators in the ipsilateral spinal dorsal horn. In HAPI microglia cell line or primary microglia, the expression of these inflammatory genes could be induced by SETD7 overexpression, or reversed by SETD7 knockdown or pharmacological inhibition of SETD7 monomethylation activity, respectively. These results indicated that SETD7 may regulate H3K4me1 marked enhancer in microglia,

which have been shown to be up-regulated and thus facilitated gene transcription after peripheral nerve injury (Denk et al., 2016), contributing to spinal microgliosis after CCI.

The up-regulation of SETD7 and H3K4me1 was maintained stable until 14 days after CCI. This is consistent with previous findings reporting that microglial enhancers may persist even one month after peripheral nerve injury (Denk et al., 2016). As H3K4me1 is enriched at enhancers, it could also act on many genes in microglia other than *Ccl2*, *Il-6* and *Il-1 β* (Denk et al., 2016). However, the expression of an individual gene in microglia may not maintain as stable as SETD7 and H3K4me1, since the nerve injury-induced gene expression is usually changed at different time and to different amounts (Denk et al., 2016; Whitehead et al., 2010). Actually, H3K4me1 marks enhancers which are composed of poised and active ones. Enrichment of H3K4me1 together with H3K27ac separate active from poised enhancers (Calo and Wysocka, 2013; Cheng et al., 2014; Ostuni et al., 2013). Although the level of H3K27ac in the spinal cord was not changed after CCI, it is possible that H3K27ac dynamically binds to a specific gene and causes temporary gene transcription (Hung et al., 2015). Besides enhancer activity, the initiation of gene transcription still requires multiple mechanisms to work together, such as recruitment of transcription factors and coactivators to initiate transcription (Lee et al., 2013). The preexisting H3K4me1-marked enhancers are required to recruit transcription factor to promote transcription of a specific gene (Heintzman et al., 2009). The continuous up-regulation of SETD7 and H3k4me1 may thus facilitate

transcription of different genes, contributing to chronic microgliosis in the spinal cord after CCI.

A previous study reported that SETD7 in the spinal cord could be involved in the development of bone cancer pain, although its effect was not directly confirmed and the underlying mechanism was not clarified (Hang et al., 2017). Our study, for the first time, demonstrates a critical role of SETD7 in spinal microgliosis and neuropathic pain after peripheral nerve injury. SETD7 knockdown led to a reduction of spinal microgliosis and attenuated neuropathic pain in CCI rats, whereas SETD7 overexpression induced significant microgliosis and pain hypersensitivity in naive rats. We further showed that PFI-2, a specific inhibitor of SETD7 monomethylation activity (Baryshte-Lovejoy et al., 2014), is effective in treating CCI-induced neuropathic pain in male but not female rats. This result is to some extent consistent with previous reports of sex-specific patterns of microglial response (Chen et al., 2018; Sorge et al., 2015; Taves et al., 2016). However, further experiments are required to determine the sex dimorphism effect of SETD7 on spinal microgliosis and neuropathic pain.

Our findings point to a chromatin-nuclear mechanism of SETD7 underlying spinal microgliosis, contributing to development of neuropathic pain. However, other than the early microgliosis, microglia in the spinal dorsal horn could remain in a chronic activation state for at least several weeks after peripheral nerve injury (Chen et al., 2018; Echeverry et al., 2017). Further experiments should be carried out to investigate whether SETD7 is involved in the chronic microglial activation and

maintenance of neuropathic pain at a later time point after peripheral nerve injury. Moreover, although SETD7-mediated monomethylation of H3K4 could be involved in regulation of inflammatory gene transcription in microglia, the exact binding profiles of H3K4me1 on these genes are elusive. For example, chromatin immunoprecipitation-sequencing to explore the genome-wide enrichment of H3K4me1 in microglia may provide further insights. In addition to H3K4me1, SETD7 also has methyltransferase activity toward non-histone proteins, such as tumor suppressor p53, ribosomal protein Rpl42ab, Rubisco LSMT, ER α , and DNMT1 (Esteve et al., 2009; Pradhan et al., 2009). Therefore, we cannot rule out at present stage that methylation of non-histone proteins by SETD7 may contribute to its function after CCI in the spinal cord. In conclusion, this study demonstrated a critical role of SETD7, presumably via monomethylation of H3K4, in the development of spinal microgliosis and neuropathic pain after CCI. The pharmacological treatment approach further suggests that SETD7 is a new target for the treatment of neuropathic pain.

5. Acknowledgement

This work was supported by National Natural Science Foundation of China (81771207, 81370027, 81873733 and 81571081) and Hunan Province Clinical Medical Technology Innovation Guide Project in 2018 (2018SK52602). The work of YS was supported by the Fundamental Research Funds for the Central Universities of Central South University (2018zzts898).

6. Author contributions

YS and ZD carried out most of the experiments and the data analysis. SM and MS participated in the study design and manuscript writing. ZD and YZ carried out the MACS and primary microglia culture. YZ and FX carried out the immunofluorescence experiments. XY participated in the data analysis. QG participated in the study conception. CH conducted the study design and drafted the final manuscript. All authors read and approved the final version of the manuscript.

7. Conflict of interests

All authors declare that they have no conflict of interest.

8. References

- Bannister, A.J., Kouzarides, T., 2011. Regulation of chromatin by histone modifications. *Cell research* 21, 381-395.
- Barsyte-Lovejoy, D., Li, F., Oudhoff, M.J., Tatlock, J.H., Dong, A., Zeng, H., Wu, H., Freeman, S.A., Schapira, M., Senisterra, G.A., Kuznetsova, E., Marcellus, R., Allali-Hassani, A., Kennedy, S., Lambert, J.P., Couzens, A.L., Aman, A., Gingras, A.C., Al-Awar, R., Fish, P.V., Gerstenberger, B.S., Roberts, L., Benn, C.L., Grimley, R.L., Braam, M.J., Rossi, F.M., Sudol, M., Brown, P.J., Bunnage, M.E., Owen, D.R., Zaph, C., Vedadi, M., Arrowsmith, C.H., 2014. (R)-PFI-2 is a potent and selective inhibitor of SETD7 methyltransferase activity in cells. *Proceedings of the National Academy of Sciences of the United States of America* 111, 12853-12858.
- Bennett, G.J., Xie, Y.K., 1988. A peripheral mononeuropathy in rat that produces disorders of pain sensation like those seen in man. *Pain* 33, 87-107.
- Bulger, M., Groudine, M., 2011. Functional and mechanistic diversity of distal transcription enhancers. *Cell* 144, 327-339.
- Calo, E., Wysocka, J., 2013. Modification of enhancer chromatin: what, how, and why? *Molecular cell* 49, 825-837.
- Calvo, M., Bennett, D.L., 2012. The mechanisms of microgliosis and pain following peripheral nerve injury. *Experimental neurology* 234, 271-282.
- Cheepsunthorn, P., Radov, L., Menzies, S., Reid, J., Connor, J.R., 2001. Characterization of a novel brain-derived microglial cell line isolated from neonatal rat brain. *Glia* 35, 53-62.

- Chen, G., Zhang, Y.Q., Qadri, Y.J., Serhan, C.N., Ji, R.R., 2018. Microglia in Pain: Detrimental and Protective Roles in Pathogenesis and Resolution of Pain. *Neuron* 100, 1292-1311.
- Chen, Y., Yang, S., Hu, J., Yu, C., He, M., Cai, Z., 2016. Increased Expression of SETD7 Promotes Cell Proliferation by Regulating Cell Cycle and Indicates Poor Prognosis in Hepatocellular Carcinoma. *PloS one* 11, e0154939.
- Cheng, J., Blum, R., Bowman, C., Hu, D., Shilatifard, A., Shen, S., Dynlacht, B.D., 2014. A role for H3K4 monomethylation in gene repression and partitioning of chromatin readers. *Molecular cell* 53, 979-992.
- Denk, F., Crow, M., Didangelos, A., Lopes, D.M., McMahon, S.B., 2016. Persistent Alterations in Microglial Enhancers in a Model of Chronic Pain. *Cell reports* 15, 1771-1781.
- Ding, Z., Cao, J., Shen, Y., Zou, Y., Yang, X., Zhou, W., Guo, Q., Huang, C., 2018. Resveratrol Promotes Nerve Regeneration via Activation of p300 Acetyltransferase-Mediated VEGF Signaling in a Rat Model of Sciatic Nerve Crush Injury. *Frontiers in neuroscience* 12, 341.
- Ding, Z., Xu, W., Zhang, J., Zou, W., Guo, Q., Huang, C., Liu, C., Zhong, T., Zhang, J.M., Song, Z., 2017. Normalizing GDNF expression in the spinal cord alleviates cutaneous hyperalgesia but not ongoing pain in a rat model of bone cancer pain. *International journal of cancer* 140, 411-422.
- Dong, X., Weng, Z., 2013. The correlation between histone modifications and gene expression. *Epigenomics* 5, 113-116.

Duan, B., Bai, J., Qiu, J., Wang, J., Tong, C., Wang, X., Miao, J., Li, Z., Li, W., Yang, J., Huang, C., 2018. Histone-lysine N-methyltransferase SETD7 is a potential serum biomarker for colorectal cancer patients. *EBioMedicine* 37, 134-143.

Ea, C.K., Baltimore, D., 2009. Regulation of NF-kappaB activity through lysine monomethylation of p65. *Proceedings of the National Academy of Sciences of the United States of America* 106, 18972-18977.

Echeverry, S., Shi, X.Q., Yang, M., Huang, H., Wu, Y., Lorenzo, L.E., Perez-Sanchez, J., Bonin, R.P., De Koninck, Y., Zhang, J., 2017. Spinal microglia are required for long-term maintenance of neuropathic pain. *Pain* 158, 1792-1801.

Esteve, P.O., Chin, H.G., Benner, J., Feehery, G.R., Samaranayake, M., Horwitz, G.A., Jacobsen, S.E., Pradhan, S., 2009. Regulation of DNMT1 stability through SET7-mediated lysine methylation in mammalian cells. *Proceedings of the National Academy of Sciences of the United States of America* 106, 5076-5081.

Ginhoux, F., Greter, M., Leboeuf, M., Nandi, S., See, P., Gokhan, S., Mehler, M.F., Conway, S.J., Ng, L.G., Stanley, E.R., Samokhvalov, I.M., Merad, M., 2010. Fate mapping analysis reveals that adult microglia derive from primitive macrophages. *Science* 330, 841-845.

Graeber, M.B., Li, W., Rodriguez, M.L., 2011. Role of microglia in CNS inflammation. *FEBS letters* 585, 3798-3805.

Graeber, M.B., Tetzlaff, W., Streit, W.J., Kreutzberg, G.W., 1988. Microglial cells but not astrocytes undergo mitosis following rat facial nerve axotomy. *Neuroscience letters* 85, 317-321.

Gu, N., Peng, J., Murugan, M., Wang, X., Eyo, U.B., Sun, D., Ren, Y., DiCicco-Bloom, E., Young, W., Dong, H., Wu, L.J., 2016. Spinal Microgliosis Due to Resident Microglial Proliferation Is Required for Pain Hypersensitivity after Peripheral Nerve Injury. *Cell reports* 16, 605-614.

Hang, L.H., Xu, Z.K., Wei, S.Y., Shu, W.W., Luo, H., Chen, J., 2017. Spinal SET7/9 may contribute to the maintenance of cancer-induced bone pain in mice. *Clinical and experimental pharmacology & physiology* 44, 1001-1007.

Harry, G.J., Kraft, A.D., 2008. Neuroinflammation and microglia: considerations and approaches for neurotoxicity assessment. *Expert opinion on drug metabolism & toxicology* 4, 1265-1277.

He, S., Owen, D.R., Jelinsky, S.A., Lin, L.L., 2015. Lysine Methyltransferase SETD7 (SET7/9) Regulates ROS Signaling through mitochondria and NFE2L2/ARE pathway. *Scientific reports* 5, 14368.

Heintzman, N.D., Hon, G.C., Hawkins, R.D., Kheradpour, P., Stark, A., Harp, L.F., Ye, Z., Lee, L.K., Stuart, R.K., Ching, C.W., Ching, K.A., Antosiewicz-Bourget, J.E., Liu, H., Zhang, X., Green, R.D., Lobanenkov, V.V., Stewart, R., Thomson, J.A., Crawford, G.E., Kellis, M., Ren, B., 2009. Histone modifications at human enhancers reflect global cell-type-specific gene expression. *Nature* 459, 108-112.

Heintzman, N.D., Stuart, R.K., Hon, G., Fu, Y., Ching, C.W., Hawkins, R.D., Barrera, L.O., Van Calcar, S., Qu, C., Ching, K.A., Wang, W., Weng, Z., Green, R.D., Crawford, G.E., Ren, B., 2007. Distinct and predictive chromatin signatures of transcriptional promoters and enhancers in the human genome. *Nature genetics* 39,

311-318.

Holt, L.M., Olsen, M.L., 2016. Novel Applications of Magnetic Cell Sorting to Analyze Cell-Type Specific Gene and Protein Expression in the Central Nervous System. *PloS one* 11, e0150290.

Huang, C., Sakry, D., Menzel, L., Dangel, L., Sebastiani, A., Kramer, T., Karram, K., Engelhard, K., Trotter, J., Schafer, M.K., 2016. Lack of NG2 exacerbates neurological outcome and modulates glial responses after traumatic brain injury. *Glia* 64, 507-523.

Hung, H.A., Sun, G., Keles, S., Svaren, J., 2015. Dynamic regulation of Schwann cell enhancers after peripheral nerve injury. *The Journal of biological chemistry* 290, 6937-6950.

Ji, R.R., Kawasaki, Y., Zhuang, Z.Y., Wen, Y.R., Decosterd, I., 2006. Possible role of spinal astrocytes in maintaining chronic pain sensitization: review of current evidence with focus on bFGF/JNK pathway. *Neuron glia biology* 2, 259-269.

Ji, R.R., Suter, M.R., 2007. p38 MAPK, microglial signaling, and neuropathic pain. *Molecular pain* 3, 33.

Judson, R.N., Quarta, M., Oudhoff, M.J., Soliman, H., Yi, L., Chang, C.K., Loi, G., Vander Werff, R., Cait, A., Hamer, M., Blonigan, J., Paine, P., Doan, L.T.N., Groppa, E., He, W., Su, L., Zhang, R.H., Xu, P., Eisner, C., Low, M., Barta, I., Lewis, C.B., Zaph, C., Karimi, M.M., Rando, T.A., Rossi, F.M., 2018. Inhibition of Methyltransferase Setd7 Allows the In Vitro Expansion of Myogenic Stem Cells with Improved Therapeutic Potential. *Cell stem cell* 22, 177-190 e177.

Lee, J.E., Wang, C., Xu, S., Cho, Y.W., Wang, L., Feng, X., Baldrige, A., Sartorelli,

V., Zhuang, L., Peng, W., Ge, K., 2013. H3K4 mono- and di-methyltransferase MLL4 is required for enhancer activation during cell differentiation. *eLife* 2, e01503.

Li, Y., Reddy, M.A., Miao, F., Shanmugam, N., Yee, J.K., Hawkins, D., Ren, B., Natarajan, R., 2008. Role of the histone H3 lysine 4 methyltransferase, SET7/9, in the regulation of NF-kappaB-dependent inflammatory genes. Relevance to diabetes and inflammation. *The Journal of biological chemistry* 283, 26771-26781.

Liu, L., Rudin, M., Kozlova, E.N., 2000. Glial cell proliferation in the spinal cord after dorsal rhizotomy or sciatic nerve transection in the adult rat. *Experimental brain research* 131, 64-73.

Maiques-Diaz, A., Somerville, T.C., 2016. LSD1: biologic roles and therapeutic targeting. *Epigenomics* 8, 1103-1116.

Marmorstein, R., Trievel, R.C., 2009. Histone modifying enzymes: structures, mechanisms, and specificities. *Biochimica et biophysica acta* 1789, 58-68.

Mika, J., Osikowicz, M., Rojewska, E., Korostynski, M., Wawrzczak-Bargiela, A., Przewlocki, R., Przewlocka, B., 2009. Differential activation of spinal microglial and astroglial cells in a mouse model of peripheral neuropathic pain. *European journal of pharmacology* 623, 65-72.

Montenegro, M.F., Sanchez-Del-Campo, L., Gonzalez-Guerrero, R., Martinez-Barba, E., Pinero-Madrona, A., Cabezas-Herrera, J., Rodriguez-Lopez, J.N., 2016. Tumor suppressor SET9 guides the epigenetic plasticity of breast cancer cells and serves as an early-stage biomarker for predicting metastasis. *Oncogene* 35, 6143-6152.

Nishioka, K., Chuikov, S., Sarma, K., Erdjument-Bromage, H., Allis, C.D., Tempst, P.,

Reinberg, D., 2002. Set9, a novel histone H3 methyltransferase that facilitates transcription by precluding histone tail modifications required for heterochromatin formation. *Genes & development* 16, 479-489.

Ostuni, R., Piccolo, V., Barozzi, I., Polletti, S., Termanini, A., Bonifacio, S., Curina, A., Prosperini, E., Ghisletti, S., Natoli, G., 2013. Latent enhancers activated by stimulation in differentiated cells. *Cell* 152, 157-171.

Peng, J., Gu, N., Zhou, L., U, B.E., Murugan, M., Gan, W.B., Wu, L.J., 2016. Microglia and monocytes synergistically promote the transition from acute to chronic pain after nerve injury. *Nature communications* 7, 12029.

Peterson, C.L., Laniel, M.A., 2004. Histones and histone modifications. *Current biology* : CB 14, R546-551.

Popiolek-Barczyk, K., Mika, J., 2016. Targeting the Microglial Signaling Pathways: New Insights in the Modulation of Neuropathic Pain. *Current medicinal chemistry* 23, 2908-2928.

Pradhan, S., Chin, H.G., Esteve, P.O., Jacobsen, S.E., 2009. SET7/9 mediated methylation of non-histone proteins in mammalian cells. *Epigenetics* 4, 383-387.

Ransohoff, R.M., Perry, V.H., 2009. Microglial physiology: unique stimuli, specialized responses. *Annual review of immunology* 27, 119-145.

Remenyi, A., Scholer, H.R., Wilmanns, M., 2004. Combinatorial control of gene expression. *Nature structural & molecular biology* 11, 812-815.

Rice, J.C., Briggs, S.D., Ueberheide, B., Barber, C.M., Shabanowitz, J., Hunt, D.F.,

Shinkai, Y., Allis, C.D., 2003. Histone methyltransferases direct different degrees of

- methylation to define distinct chromatin domains. *Molecular cell* 12, 1591-1598.
- Shemer, A., Erny, D., Jung, S., Prinz, M., 2015. Microglia Plasticity During Health and Disease: An Immunological Perspective. *Trends in immunology* 36, 614-624.
- Sorge, R.E., Mapplebeck, J.C., Rosen, S., Beggs, S., Taves, S., Alexander, J.K., Martin, L.J., Austin, J.S., Sotocinal, S.G., Chen, D., Yang, M., Shi, X.Q., Huang, H., Pillon, N.J., Bilan, P.J., Tu, Y., Klip, A., Ji, R.R., Zhang, J., Salter, M.W., Mogil, J.S., 2015. Different immune cells mediate mechanical pain hypersensitivity in male and female mice. *Nature neuroscience* 18, 1081-1083.
- Tao, Y., Nepl, R.L., Huang, Z.P., Chen, J., Tang, R.H., Cao, R., Zhang, Y., Jin, S.W., Wang, D.Z., 2011. The histone methyltransferase Set7/9 promotes myoblast differentiation and myofibril assembly. *The Journal of cell biology* 194, 551-565.
- Taves, S., Berta, T., Liu, D.L., Gan, S., Chen, G., Kim, Y.H., Van de Ven, T., Laufer, S., Ji, R.R., 2016. Spinal inhibition of p38 MAP kinase reduces inflammatory and neuropathic pain in male but not female mice: Sex-dependent microglial signaling in the spinal cord. *Brain, behavior, and immunity* 55, 70-81.
- Tsuda, M., Koga, K., Chen, T., Zhuo, M., 2017. Neuronal and microglial mechanisms for neuropathic pain in the spinal dorsal horn and anterior cingulate cortex. *Journal of neurochemistry* 141, 486-498.
- Tuano, N.K., Okabe, J., Ziemann, M., Cooper, M.E., El-Osta, A., 2016. Set7 mediated interactions regulate transcriptional networks in embryonic stem cells. *Nucleic acids research* 44, 9206-9217.
- US National Research Council, 1996. *Guide for the Care and Use of Laboratory*

Animals. National Academy Press, Washington (DC).

Whitehead, K.J., Smith, C.G., Delaney, S.A., Curnow, S.J., Salmon, M., Hughes, J.P., Chessell, I.P., 2010. Dynamic regulation of spinal pro-inflammatory cytokine release in the rat in vivo following peripheral nerve injury. *Brain, behavior, and immunity* 24, 569-576.

Xu, F., Huang, J., He, Z., Chen, J., Tang, X., Song, Z., Guo, Q., Huang, C., 2016a. Microglial polarization dynamics in dorsal spinal cord in the early stages following chronic sciatic nerve damage. *Neuroscience letters* 617, 6-13.

Xu, J., Li, L., Xiong, J., denDekker, A., Ye, A., Karatas, H., Liu, L., Wang, H., Qin, Z.S., Wang, S., Dou, Y., 2016b. MLL1 and MLL1 fusion proteins have distinct functions in regulating leukemic transcription program. *Cell discovery* 2, 16008.

Xu, M., Cheng, Z., Ding, Z., Wang, Y., Guo, Q., Huang, C., 2018. Resveratrol enhances IL-4 receptor-mediated anti-inflammatory effects in spinal cord and attenuates neuropathic pain following sciatic nerve injury. *Molecular pain* 14, 1744806918767549.

Zhang, K., Dent, S.Y., 2005. Histone modifying enzymes and cancer: going beyond histones. *Journal of cellular biochemistry* 96, 1137-1148.

Zhu, X.Y., Huang, C.S., Li, Q., Chang, R.M., Song, Z.B., Zou, W.Y., Guo, Q.L., 2012. p300 exerts an epigenetic role in chronic neuropathic pain through its acetyltransferase activity in rats following chronic constriction injury (CCI). *Molecular pain* 8, 84.

Figure legends**Figure 1: CCI induces neuropathic pain and up-regulates expression of SETD7 protein and inflammatory genes in spinal dorsal horn ipsilateral to nerve lesion.**

Rats developed neuropathic pain, manifested as decreased mechanical withdrawal threshold (MWT) (A) and thermal withdrawal latency (TWL) (B) on the ipsilateral paw. Measurements were performed before surgery (BS) and at 1 day (d), 3d, 7d, and 14d after CCI or sham surgery. Compared to sham-operated rats, $*p < 0.05$, $**p < 0.01$, $***p < 0.001$, $n = 8$, two-way ANOVA with repeated measures followed by Bonferroni multiple comparison test. Western blot analysis of nuclear protein showed the expression of SETD7 was increased in the ipsilateral spinal dorsal horn (C) but not the ipsilateral L4-L5 dorsal root ganglions (DRGs) (D) after CCI. Measurements were performed at 12 hours (h), and at 1d, 3d, 7d, and 14d after CCI or sham surgery. The protein expression was relative to the level of H3. Compared to sham-operative rats, $*p < 0.05$, $n = 4$, one-way ANOVA followed by Bonferroni's multiple comparison test. (E) The expression of inflammatory genes, including *Ccl2*, *Il-6* and *Il-1 β* , were increased in the ipsilateral spinal dorsal horn from 1d to 14d after CCI. Compared to sham-operative rats, $*p < 0.05$, $**p < 0.01$, $***p < 0.001$, $n = 6$, one-way ANOVA followed by Bonferroni's multiple comparison test.

Figure 2: CCI-induced expression of SETD7 protein is localized to ipsilateral spinal dorsal horn microglia. Analyses were made at seven days after sham-operated or CCI surgery.

(A) Representative images showed the co-localization of SETD7 with Iba1, a marker of microglia in the ipsilateral spinal dorsal horn of the sham-operative rats and CCI rats. Microgliosis were observed in CCI rats, demonstrating as microglial proliferation and morphological change from ramified cells (sham) to hypertrophied and amoeboid cells (CCI). Arrow heads: SETD7 co-localized with only a part of Iba1-labeled microglia in sham-operated rats but co-localized with almost Iba1-labeled microglia in CCI rats. Scale bar = 100 μm . (B) Ratio of SETD7 positive / Iba1 positive (SETD7⁺ / Iba1⁺) microglia were increased in the ipsilateral spinal dorsal horn (laminae I–V) after CCI. Compared to sham-operated rats, ** $p < 0.01$, $n = 6$, two-tailed unpaired Student's t-test. (C) Representative images showed the localization of SETD7 positive staining in the nuclear (labeled with DAPI) of Iba1-labeled microglia in the sham-operated rats and CCI rats, respectively. Scale bar = 50 μm . (D) Western blot analysis of the positive fraction and negative fraction of the ipsilateral spinal dorsal horn separated using anti-CD11b/c magnetic cell sorting. CD11b protein was expressed in positive fraction but not negative fraction, indicating a successful separation. Compared to sham-operated rats, CD11b and SETD7 were increased in the positive fraction of the ipsilateral spinal dorsal horn of CCI rats. The protein expression was relative to the level of H3. *** $p < 0.001$, $n = 3$, two-tailed unpaired Student's t-test.

Figure 3: SETD7 knockdown suppresses spinal microgliosis and alleviates CCI-induced neuropathic pain.

(A) Western blot analysis showed that the expression of SETD7 in the ipsilateral spinal dorsal horn of CCI rats was inhibited by lentivirus (LV)-shRNA (Data were collected at 14 days after CCI or sham-operated surgery. CCI + normal saline (NS) vs sham + NS, $*p < 0.05$; CCI + LV-shRNA vs CCI + LV-negative control (NC), $*p < 0.05$, $n = 4$, one-way ANOVA followed by Bonferroni's multiple comparison test). (B) Inhibition of SETD7 by LV-shRNA suppressed the increasing fluorescence density of Iba1-labeled microglia in the ipsilateral spinal dorsal horn (Data were collected at 14 days after CCI or sham-operated surgery. CCI + NS vs sham + NS, $*p < 0.05$; CCI + LV-shRNA vs CCI + LV- NC, $*p < 0.05$, $n = 4$, Kruskal–Wallis test with Dunn's multiple comparisons post-test). Scale bar = 100 μm . (C) Analysis using enzyme-linked immunosorbent assay showed that the CCI-induced expression of CCL2, IL-6 and IL-1 β were down-regulated after SETD7 knockdown (Data were collected at 14 days after CCI or sham-operated surgery. CCI + NS vs sham + NS, $**p < 0.01$, $***p < 0.001$, CCI + LV-shRNA vs CCI + LV-NC, $**p < 0.01$, $n = 6$, one-way ANOVA followed by Bonferroni's multiple comparison test). (D) Inhibition of SETD7 by intrathecal injection of LV-shRNA 7 days before CCI prevented the CCI-induced decrease of mechanical withdrawal threshold (MWT) and thermal withdrawal latency (TWL) on the ipsilateral paw. MWT and TWL were measured on the day when the intrathecal treatment was performed and repeated on the day for performing CCI and 1, 3, 7 and 14 days thereafter (CCI + NS vs sham + NS, $***p < 0.001$; CCI + LV-shRNA vs CCI + LV- NC, $^{\#}p < 0.05$, $^{\#\#}p < 0.01$, $^{\#\#\#}p < 0.001$, $n = 8$, two-way ANOVA with repeated measures followed by Bonferroni multiple

comparison test).

Figure 4: SETD7 overexpression causes spinal microgliosis and pain hypersensitivity in naive rats.

(A) LV-SETD7 increased the protein level of SETD7 in the spinal dorsal horn (LV-SETD7 vs control, $n = 4$, $*p < 0.05$, two-tailed unpaired Student's t-test. Data were collected at 14 days after the LV transfection). (B) LV-SETD7 increased the fluorescence density of Iba1-labeled microglia in the spinal dorsal horn (LV-SETD7 vs control, $**p < 0.01$, $n = 4$, two-tailed unpaired Student's t-test. Data were collected at 14 days after LV transfection). Scale bar = 100 μm . (C) Intrathecal injection of LV-SETD7 to the lumbar spinal cord decreased the mechanical withdrawal threshold (MWT) and thermal withdrawal latency (TWL) on the hindpaw (LV-SETD7 vs control, $**p < 0.01$, $***p < 0.001$, $n = 8$, two-way ANOVA with repeated measures followed by Bonferroni multiple comparison test).

Figure 5: SETD7 up-regulates monomethylation level of H3K4 in ipsilateral spinal dorsal horn microglia after CCI

(A - D) Western blot analysis of nuclear protein showed the expression of H3K4me1, H3K4me3 and H3K27ac in the ipsilateral spinal dorsal horn of sham-operated rats and CCI rats at 12 hours (h), and at 1 day (d), 3d, 7d, and 14d after surgery, respectively. Representative bands of protein expression (A). Protein expression of H3K4me1 (B), H3K4me3 (C) and H3K27ac (D) relative to the level of H3.

Compared to sham-operative rats, $*p < 0.05$, $n = 4$, one-way ANOVA followed by Bonferroni's multiple comparison test. (E) Representative images at 7d post injury showed the co-localization of H3K4me1 with Iba1-labeled microglia in the ipsilateral spinal dorsal horn of the sham-operative rats and CCI rats. Arrow heads: H3K4me1 co-localized with only a part of Iba1-labeled microglia in sham-operated rats but co-localized with almost Iba1-labeled microglia in CCI rats. Scale bar = 100 μm . (F) Ratio of H3K4me1 positive / Iba1 positive ($\text{H3K4me1}^+ / \text{Iba1}^+$) microglia were increased in the ipsilateral spinal dorsal horn (laminae I–V) after CCI. Compared to sham-operated rats, $***p < 0.001$, $n = 6$, two-tailed unpaired Student's t-test. (G) Western blot analysis of the positive fraction and negative fraction of the ipsilateral spinal dorsal horn separated using anti-CD11b/c magnetic cell sorting. Data were collected at 7d post injury. H3K4me1 was significantly higher in the positive fraction of CCI rats. Compared to sham-operated rats, $**p < 0.01$, $n = 3$, two-tailed unpaired Student's t-test. (H) Representative images at 7d post injury showed the co-localization of SETD7 and H3K4me1 in the ipsilateral spinal dorsal horn after CCI. Scale bar = 50 μm . (I) Western blot analysis showed that the expression of H3K4me1 in the ipsilateral spinal dorsal horn of CCI rats was inhibited by SETD7 knockdown with lentivirus (LV)-shRNA (Data were collected at 14d post injury. CCI + normal saline (NS) vs sham + NS, $*p < 0.05$; CCI + LV-shRNA vs CCI + LV-negative control (NC), $*p < 0.05$, $n = 4$, one-way ANOVA with Bonferroni multiple comparison test). (J) Western blot analysis showed that the expression of H3K4me1 in the spinal dorsal horn was increased by SETD7 overexpression with

LV-SETD7 (Data were collected at 14d after LV transfection. LV-SETD7 vs control, $*p < 0.05$, $n = 4$, two-tailed unpaired Student's t-test).

Figure 6: SETD7 controls monomethylation level of H3K4 and inflammatory gene expression in HAPI microglia

(A) Representative images showed the labeling of Iba1 (a microglial marker) in HAPI cells (identified by DAPI, a marker of cell nuclei). Scale bar = 100 μm . (B) The expression of *SETD7* was dramatically reduced by LV-shRNA. Compared to negative control (NC), $***p < 0.001$, $n = 4$, two-tailed unpaired Student's t-test. (C) SETD7 knockdown by LV-shRNA suppressed the lipopolysaccharides (LPS)-increased level of H3K4me1 (LPS vs control, $*p < 0.05$; LPS + LV-shRNA vs LPS + LV-negative control (NC), $**p < 0.01$, $n = 4$, one-way ANOVA with Bonferroni multiple comparison test). (D) SETD7 knockdown by LV-shRNA suppressed the LPS-induced expression of inflammatory genes *Ccl2*, *Il-6* and *Il-1 β* (LPS vs control, $*p < 0.05$; LPS + LV-shRNA vs LPS + LV- NC, $*p < 0.05$, $n = 4$, Kruskal–Wallis test with Dunn's multiple comparisons post-test). (E) SETD7 overexpression via LV transfection (LV-SETD7) enhanced the protein level of SETD7 and H3K4me1 in HAPI microglia (LV-SETD7 vs control, $**p < 0.01$, $n = 4$, two-tailed unpaired Student's t-test). (F) LV-SETD7 up-regulated the expression of inflammatory genes *Ccl2*, *Il-6* and *Il-1 β* in HAPI microglia (LV-SETD7 vs control, $**p < 0.01$, $***p < 0.001$, $n = 4$, two-tailed unpaired Student's t-test).

Figure 7 Inhibition of SETD7 monomethylation activity suppresses LPS-induced expression of inflammatory genes in primary microglia

(A) Representative images showed that pre-treatment of PFI-2 prevented the LPS-induced morphological transformation of primary microglia. The resting microglia (Blank) showed a ramified morphology, whereas the microglia after LPS treatment showed an amoeboid morphology. Treatment of PFI-2 (0.1 μmol) but not the vehicle prevented the LPS (0.1 $\mu\text{g/ml}$)-induced morphological change of microglia. Scale bar = 100 μm . (B) The LPS-induced expression of inflammatory genes, *Ccl2*, *Il-6* and *Il-1 β* , were attenuated by PFI-2 treatment (LPS vs Blank, $***p < 0.001$, PFI-2 + LPS vs vehicle + LPS, $**p < 0.01$, $***p < 0.001$, $n = 3$, one-way ANOVA with Bonferroni multiple comparison test).

Figure 8: Inhibition of SETD7 monomethylation activity alleviates CCI-induced neuropathic pain

Vehicle or PFI-2 (1 μmol , 4 μmol or 10 μmol) were intrathecally injected once daily from the day when sham or CCI surgery was performed to the next 14 days. The mechanical withdrawal threshold (MWT) (A) and thermal withdrawal latency (TWL) (B) on the ipsilateral paw were measured (CCI + vehicle vs sham + vehicle, $*p < 0.05$, $***p < 0.001$; CCI + 4 μmol PFI-2 vs CCI + vehicle, $###p < 0.001$ for TWL at 14 days after CCI; CCI + 10 μmol PFI-2 vs CCI + vehicle, $##p < 0.01$ for MWT at 3, 7 and 14 days after CCI, $###p < 0.001$ for TWL at 7 and 14 days after CCI, respectively, $n = 6$, two-way ANOVA with repeated measures followed by Bonferroni multiple

comparison test).

Highlights

Expression of SETD7 increases in spinal microglia after CCI.

SETD7 contributes to spinal microgliosis subsequent to CCI.

SETD7 regulates H3K4me1 level and expression of inflammatory genes in microglia.

Genetic or pharmacological inhibition of SETD7 prevented CCI-induced neuropathic pain.